Polymer 316 (2025) 127861

Contents lists available at ScienceDirect

Polymer

journal homepage: www.elsevier.com/locate/polymer

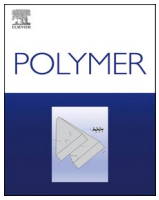

Anionic polymers formed by dinuclear rhodium units and dicyanide silver/gold moieties

Laura Abad Galán [a,**], Paula Cruz [a], Estefanía Fernández-Bartolomé [a], Miguel Cortijo [a], Patricia Delgado-Martínez [b], Rodrigo González-Prieto [a], Reyes Jiménez-Aparicio [a], José L. Priego [a,*]

[a] Departamento de Química Inorgánica, Facultad de Ciencias Químicas, Universidad Complutense de Madrid, Ciudad Universitaria, E-28040, Madrid, Spain
[b] Unidad de Difracción de Rayos X, Centro de Asistencia a la Investigación de Técnicas Químicas, Universidad Complutense de Madrid, Ciudad Universitaria, E-28040, Madrid, Spain

A B S T R A C T

The synthesis, characterization and structural determination of four complexes with formula $(PPh_4)_n\{[Rh_2(\mu\text{-}O_2CPh)_4][Au(CN)_2]\}_n$ (**1**) and $K_n\{[Rh_2(\mu\text{-}O_2CR)_4][M(CN)_2]\}_n$ (M = Au, R =CH_2OEt (**2**), CH_2OMe (**3**); M = Ag, R =CH_2OMe (**4**)) are described. In all cases, the $[CN\text{-}M\text{-}CN]^-$ (M = Au, Ag) group is bridging the axial positions of the dirhodium units giving one-dimensional chains. The packing of the chains in the solid state depends on the nature of the carboxylate group of the dimetallic unit, the counterion present in the complex and the metal itself. The most striking change is observed in the $K_n\{[Rh_2(\mu\text{-}O_2CCH_2OMe)_4][Au(CN)_2]\}_n$ complex (**3**), where the chains are positioned perpendicular to each other with an Au···Au interchain distance of 2.963 Å. The emission studies of this complex upon excitation at 350 nm show a clear broad emission band centered at 430 nm, while no luminescence is observed for the other compounds. The appearance of emission properties only in the case of complex **3** can be explained by its short aurophilic interactions.

1. Introduction

The study of coordination polymers assembled from metal-organic building blocks has become a very fruitful research area within the inorganic and coordination chemistry fields [1–3]. A proper choice of metal ions and ligands together with a fine-control of the dimensionality and topology of the resulting materials allow targeting a vast range of novel properties and potential applications [4–9]. Additionally, the incorporation of two or more metal ions in a controlled fashion opens unique perspectives to obtain a plethora of interesting functionalities [10–13]. Heterometallic rhodium-silver and rhodium-gold compounds with interesting properties as luminescence [14,15] or catalysis [16–18] are used to this purpose.

Paddlewheel dirhodium tetracaboxylates, $[Rh_2(\mu\text{-}O_2CR)_4(L_{axial})_2]$, have been substantially studied mainly owing to their applications in different fields such as catalysis [19–22], sensors [23–25] or biomedicine [26–28]. For example, the incorporation of dirhodium paddlewheel units into proteins allows the development of new heterogeneous catalysts [29]. These tetracarboxylatodirhodium compounds are formed by a Rh_2^{4+} unit, whose molecular orbital diagram hold 14 valence electrons in a $\sigma^2\pi^4\delta^2\delta^{*2}\pi^{*4}$ configuration, leading to a diamagnetic unit and a single metal-metal bond.

Dirhodium tetracaboxylates are, in addition, appealing scaffolds to rationally construct one-dimensional coordination polymers. Their axial positions are usually occupied by neutral labile molecules of solvent, which can be readily replaced by appropriate bridging ligands acting as linkers to construct polymers arranged from an infinite array of paddlewheel units [30–34]. Among those linkers, dicyanoaurate, $[Au(CN)_2]^-$, and dicyanoargentate, $[Ag(CN)_2]^-$, have been employed in the past by our research group to prepare anionic heterometallic coordination polymers [35–37]. It must be noted that, in principle, dicyanoaurate fragments could induce luminescent properties in the resulting materials arising from their aurophilicity [38]. We have observed that the compounds $K_n\{[Rh_2(\mu\text{-}O_2CR)_4][Au(CN)_2]\}_n$ (R = Et, Me) form non-linear polymeric chains in the solid state and present similar structural parameters [35]. However, this simple modification results in a dramatic change in their luminescent properties. While the complex with the ethyl substituent displays aurophilic interactions and luminescent behavior these properties are absent in the complex with methyl groups. In contrary, the series of $(PPh_4)_n\{[Rh_2(\mu\text{-}O_2CR)_4][Au(CN)_2]\}_n$ (R = Me, CH_2OMe, CH_2OEt) complexes do not show luminescence properties probably due to the presence of the bulky

* Corresponding author.
** Corresponding author.
E-mail addresses: laabad03@ucm.es (L.A. Galán), bermejo@ucm.es (J.L. Priego).

https://doi.org/10.1016/j.polymer.2024.127861
Received 5 June 2024; Received in revised form 8 October 2024; Accepted 18 November 2024
Available online 20 November 2024

tetraphenylphosphonium counter-ion which prevents the approach of the chains [37]. In summary, between all the derivatives with [Au(CN)$_2$]$^-$ groups only one complex, K$_n${[Rh$_2$(μ-O$_2$CEt)$_4$][Au(CN)$_2$]}$_n$, displays luminescence. Also, a series of similar compounds with [Ag(CN)$_2$]$^-$ it has been described showing similar wavy chains [36].

In the present work a more detailed study is carried out to better understand the appearance of luminescence in this type of complexes. Thus, the synthesis, characterization and structural determination of three new gold complexes with formula (PPh$_4$)$_n${[Rh$_2$(μ-O$_2$CPh)$_4$][Au(CN)$_2$]}$_n$ (**1**) and K$_n${[Rh$_2$(μ-O$_2$CR)$_4$][M(CN)$_2$]}$_n$ (M = Au, R =CH$_2$OEt (**2**), CH$_2$OMe (**3**)) are described. The analysis of the different counter-ions (K$^+$ or PPh$_4^+$) and the nature of the bridging ligand in the dirhodium unit (CH$_2$OMe, CH$_2$OEt or Ph) are analyzed to explain the properties of these compounds. We have chosen the O$_2$CCH$_2$OMe, O$_2$CCH$_2$OEt ligands due to the presence of flexible chains with O atoms that favor intermolecular interactions. These interactions can be important in the approximation of the chains. We have also chosen the ligand O$_2$CPh and the counterion PPh$_4^+$ because the phenyl ring can give rise to π-π interactions. The influence of these factors in the Au···Au distance and in the presence of luminescence is also studied. Finally, an analogous complex to **3** was also studied using Ag in place of Au to study the influence of the metal in the packing of the chains and verify the lower tendency of silver to form metallophilic interactions and the absence of luminescence**.**

2. Experimental section

2.1. Materials

All the starting compounds were synthesized following previously reported procedures [36,37]: [Rh$_2$(μ-O$_2$CCH$_2$OMe)$_4$(thf)$_2$], [Rh$_2$(μ-O$_2$CCH$_2$OEt)$_4$(thf)$_2$], [Rh$_2$(μ-O$_2$CPh)$_4$(OEt$_2$)$_2$], PPh$_4$[Au(CN)$_2$]. The [Rh$_2$(μ-O$_2$CCH$_3$)$_4$], K[Au(CN)$_2$] and K[Ag(CN)$_2$] compounds were directly used from commercial sources.

2.2. Physical measurements

The elemental analysis measurements were carried out at the Microanalytical Services of the Complutense University of Madrid. Mass spectra were conducted at the Mass Spectrometry Research Asistant Centre (RAC) of the UCM by ElectroSpray Ionization technique using a Bruker Esquire-L ion trap mass spectrometer. The ^{1}H NMR spectra were carried out at the Nuclear Magnetic Resonance and Electronic Spin RAC of the UCM using a Bruker DPX-300MHz-BACS-60. FTIR measurements were performed in the 4000 to 650 cm^{-1} spectral range with a Perkin–Elmer Spectrum 100 equipped with a universal ATR accessory (PerkinElmer, Inc., Shelton, CT, USA). The diffuse reflectance spectrum of **3** was recorded on a Cary 5G spectrophotometer equipped with a Praying Mantis accessory. The absorption spectrum was then calculated by applying the Kubelka-Munk (KM) function: F(R) = α/S = (1-R)^2/2R, where α is the absorption coefficient, S is the scattering coefficient, considered wavelength independent for particle sizes larger than 5 μm, and R is reflectance. The emission spectrum of **3** was recorded at room temperature with a HORIBA Fluoromax and the excitation spectra with a Gilden Photonics fluoroSENS TCSPC Steady-State Fluorescence Spectrometers. The sample powder (approximately 30 mg) was mounted on a cell with a quartz window and irradiated at a 54.7-degree angle relative to the surface to minimize the scattering of the sample.

2.3. Crystallography

Single-crystal X-ray diffraction measurements of **1**–**4**, were carried out at room temperature using a Bruker Smart-CCD diffractometer (Bruker Corporation, Billerica, MA, USA) with a Mo Kα (λ = 0.71073 Å) radiation and a graphite monochromator. CCDC **2309412–2309415** contain the crystallographic data for the compounds described in this article. These data can be obtained free of charge from the Cambridge Crystallographic Data Centre via www.ccdc.cam.ac.uk/data_request/cif. More detailed information can be found in Figs. S1–S4 and Tables S1–S12 in the Supplementary Material.

2.4. Synthesis

2.4.1. *(PPh$_4$)$_n${[Rh$_2$(μ-O$_2$CPh)$_4$][Au(CN)$_2$]}$_n$·* ***(1)***

A 0.1 mmol (0.08 g) solution of [Rh$_2$(μ-O$_2$CPh)$_4$(OEt$_2$)$_2$] in 10 mL CH$_2$Cl$_2$ was prepared. Then a 0.1 mmol (0.06 g) solution of PPh$_4$[Au(CN)$_2$] in 8 mL CH$_2$Cl$_2$ was added. As soon as the solutions were mixed, a colour change from green to purple was observed and a precipitate appeared. Upon 24 h of stirring, the solid was filtered and dried, and the compound **1·CH$_2$Cl$_2$** is obtained in a 59 % yield (80 mg). Anal. Calcd. ((PPh$_4$)$_n${[Rh$_2$(μ-O$_2$CPh)$_4$][Au(CN)$_2$]·CH$_2$Cl$_2$}$_n$): C, 48.45; H, 3.10; N, 2.05. Found (%): C, 48.51; H, 3.11; N, 2.35. FT-IR (cm^{-1}): 3059 w, 2163 w, 1603 s, 1564 s, 1493 w, 1484 w, 1437 m, 1394 s, 1172 m, 1107 s, 1070 m, 1026 m, 996 m, 845 m, 753 m, 715 s, 689 s. ESI$^-$: *m/z* = 248.6 [Au(CN)$_2$]$^-$. In this case only this peak is clearly observed. ^{1}H NMR (500 MHz, DMSO, *δ* (ppm)): 7.64 (m, 40H). Single crystals suitable for X-Ray diffraction were obtained by dissolving the compound in acetone and adding hexane to form a double phase, allowing the mixture to diffuse for 7 days at 6 °C.

2.4.2. *K$_n${[Rh$_2$(μ-O$_2$CCH$_2$OEt)$_4$][Au(CN)$_2$]}$_n$* ***(2)***

A solution of 0.08 mmol (0.06 g) of [Rh$_2$(μ-O$_2$CCH$_2$OEt)$_4$(thf)$_2$] in 15 mL H$_2$O was prepared. Then a 0.1 mmol (0.03 g) solution of K[Au(CN)$_2$] in 5 mL H$_2$O was added. As soon as the solutions were mixed, a change in colour from green to purple was observed. The reaction was stirred for 24 h and the product was obtained by removing the solvent under reduced pressure. A purple powdery solid corresponding to **2·H$_2$O** was obtained with a 62 % yield (46 mg). Anal. Calcd. (K$_n${[Rh$_2$(μ-O$_2$CCH$_2$OEt)$_4$][Au(CN)$_2$]·H$_2$O}$_n$): C, 23.39; H, 3.27; N, 3.03. Found (%): C, 23.25; H, 3.02; N, 3.32. FT-IR (cm^{-1}): 2971 w, 2932 w, 2881 w, 2160 w, 1604 s, 1459 m, 1429 s, 1369 w, 1327 s, 1302 m, 1180 m, 1108 s, 1041 m, 1019 m, 945 w, 890 m, 808 w, 734 s. ESI$^-$, *m/z* = 866.8 {[Rh$_2$(μ-O$_2$CCH$_2$OEt)$_4$][Au(CN)$_2$]}$^-$. ^{1}H NMR (500 MHz, DMSO, *δ* (ppm)): 3.79 (s, 8H), * (q, 8H), 1.02 (t, 12H). *The frequency and integration of the signal assigned to the quadruplet could not be determined as it overlaps with the solvent signal. Single crystals suitable for single crystal X-ray diffraction were obtained by evaporation at room temperature of a solution of the product in MeOH.

2.4.3. *K$_n${[Rh$_2$(μ-O$_2$CCH$_2$OMe)$_4$][Au(CN)$_2$]}$_n$* ***(3)***

0.28 mmol (0.20 g) of [Rh$_2$(μ-O$_2$CCH$_2$OMe)$_4$(thf)$_2$] were dissolved in 10 mL MeOH and 0.30 mmol (0.10 g) of K[Au(CN)$_2$] in 5 mL H$_2$O. Upon mixture in a round-bottomed flask with stirring, a purple precipitate was formed immediately. After 30 min, the precipitate was filtered, washed with 15 mL of H$_2$O and 10 mL Et$_2$O and dried to vacuum. A purple solid corresponding to **3·H$_2$O** was obtained in 43 % yield (104 mg). Anal. Calcd. (K$_n${[Rh$_2$(μ-O$_2$CCH$_2$OMe)$_4$][Au(CN)$_2$]H$_2$O}$_n$): C, 19.37; H, 2.55; N, 3.23. Found (%): C, 19.07; H, 2.44; N, 3.60. FT-IR (cm^{-1}): 2898 w, 2826 w, 2162 w, 1602 s, 1432 m, 1411 m, 1341 m, 1332 m,1208 w, 1199 w, 1117 s, 1019 w, 984 w, 938 w, 920 w, 744 s. ESI$^-$: *m/z* = 248.6 [Au(CN)$_2$]$^-$, 810.3 {[Rh$_2$(μ-O$_2$CCH$_2$OMe)$_4$][Au(CN)$_2$]}$^-$. ^{1}H NMR: (500 MHz, DMSO, *δ*(ppm)): 3.79 (s, 8H), 3.11 (s, 12H). Some single crystals of **3** were obtained by a double step by dissolving 0.18 mmol (0.10 g) of [Rh$_2$(μ-O$_2$CCH$_2$OMe)$_4$] in 5 mL MeOH and 0.18 mmol (0.05 g) of K[Au(CN)$_2$] in 2 mL H$_2$O. The potassium dicyanoaurate solution is placed in a test tube and the [Rh$_2$(μ-O$_2$CCH$_2$OMe)$_4$] solution is placed on top of it in a double phase.

2.4.4. *K$_n${[Rh$_2$(μ-O$_2$CCH$_2$OMe)$_4$][Ag(CN)$_2$]}$_n$* ***(4)***

The reaction is similar to that described for **3**.0.28 mmol (0.20 g) of [Rh$_2$(μ-O$_2$CCH$_2$OMe)$_4$ (thf)$_2$] and 0.30 mmol (0.07 g) of K[Ag(CN)$_2$] were dissolved in 5 mL of EtOH and 5 mL of H$_2$O, respectively. Both

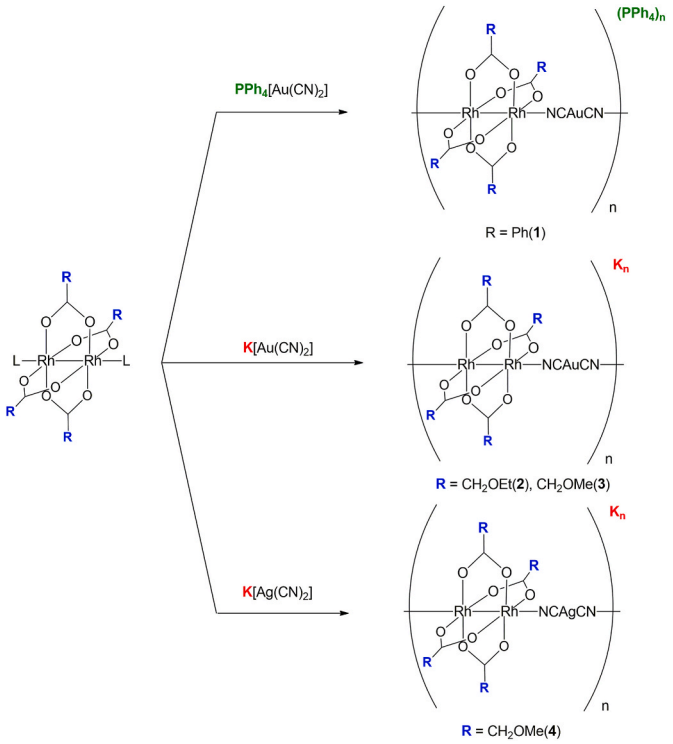

Fig. 1. Synthetic approach for the preparation of compounds **1**–**4**.

solutions were mixed and stirred and a purple precipitate was formed. After half an hour of reaction, the product formed was filtered, washed with EtOH and H_2O and dried to vacuum. A purple solid of **4·2H$_2$O** was obtained in a 44 % yield (94 mg). Anal. Calcd. (K_n{[Rh_2(μ-$O_2CCH_2OMe)_4$][$Ag(CN)_2$]·$2H_2O$}$_n$): C, 21.10; H, 3.03; N, 3.51. Found (%): C, 20.87; H, 2.62; N, 3.86. FT-IR (cm^{-1}): 3573 w, 2824 w, 2161w 1998 w, 1600 vs, 1431 m, 1412 m, 1338 m,1200 m, 1115 s, 1021 w, 992 w, 937 w, 919 w, 741 s. ESI$^-$, m/z = 722.6 {[Rh_2(μ-$O_2CCH_2OMe)_4$][$Ag(CN)_2$]}$^-$. ^{1}H NMR (500 MHz, DMSO, δ(ppm)): 3.79 (s, 8H), 3.11 (s, 12H). The purple solid was dissolved in 4 mL ethanol and diethyl ether was added in a double phase. After 96 h, violet single crystals suitable for X-ray diffraction were obtained corresponding to K_n{[Rh_2(μ-$O_2CCH_2OMe)_4$][$Ag(CN)_2$]}$_n$

3. Results and discussion

3.1. Synthesis and structural characterization

The synthesis of the molecular threads has been performed by connecting the [Rh_2(μ-$O_2CR)_4$] (R═CH_2OMe, CH_2OEt or Ph) units with the corresponding linkers, [$M(CN)_2$]$^-$, being M = Au, Ag (Fig. 1). The differences in structural distribution according to the carboxylate ligand employed, the counteranion used (K^+ or PPh_4^+) and the metal of the linker were studied.

In all compounds, the elemental analysis of carbon, hydrogen and nitrogen is in agreement with the proposed stoichiometries (with or without a molecule of solvent). All the IR spectra of the compounds present the symmetric and antisymmetric stretching bands characteristic of these ligands: $\nu(COO_{as})$ 1610-1550 cm^{-1}, $\nu(COO_{sym})$ 1450-1400 cm^{-1}. In addition, bands characteristic of aliphatic ν(CH) stretching vibration are found below 3000 cm^{-1}. Aromatic ν(CH) tensions above this frequency are present in compound **1** due to the presence of phenyl groups both in the R = Ph and the tetraphenylphosphonium group. All complexes also present the ν(CN) bands between 2160 and 2163 cm^{-1}. This narrow range indicates the null influence of the coordination environment of K^+ counterion in the CN stretching band suggesting a weak bonding interaction. Moreover, these bands are displaced to higher energies than those of the K[$Ag(CN)_2$] and K[$Au(CN)_2$] starting materials (2132 and 2140 cm^{-1}, respectively). This shift is a general trend observed in bridged cyano complexes of the type M-C ≡ N-M', probably due to an electronic donation from the dirhodium unit [39]. The mass spectra of compounds **1**–**4** were recorded using electrospray ionization (ESI) in negative mode. Compounds **2**–**4** present the characteristic peaks for {[Rh_2(μ-$O_2CR)_4$][$M(CN)_2$]}$^-$ fragments. These type of heterometallic fragments exits in the solid state but disappears in solution with donor solvents. However, similar fragments have been previously observed in analogous compounds [36] and are probably formed by recombination of fragments during the spectrum recording [40]. In the case of **1** only the [$Au(CN)_2$]$^-$ was observed. Finally, the ^{1}H NMR spectrum was recorded for all complexes in DMSO-d_6, whose coordinative power should break the Rh–N axial bond. Complex **1** display a multiplet at 7.64 ppm assigned to the aromatic protons of the phenyl group of the carboxylate ligands and the PPh_4^+ cations. Complex **2**, presents three signals: a singlet at 3.79 ppm assigned to the CH_2 of the carboxylate group and a quadruplet and a triplet corresponding to the ethoxy group of the ligand with signals centered at ~2.5 ppm (which overlaps with the solvent signal) and 1.02 ppm, respectively. Complexes **3** and **4** present two distinguished singlets at 3.79 ppm and 3.11 ppm integrating for 8 and 12 protons, respectively. They can be assigned to the CH_2 and CH_3 of the four methoxy acetate ligands.

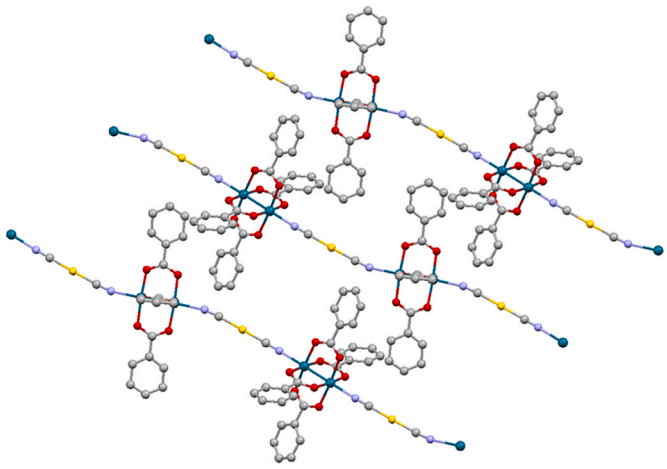

Fig. 2. View of the structure of **1**. Rh atoms are shown in turquoise, O atoms in red, C atoms in grey, N atoms in light purple, and Au atoms in yellow. H atoms and PPh_4^+ cations are omitted for the sake of clarity. (For interpretation of the references to colour in this figure legend, the reader is referred to the Web version of this article.)

3.2. Crystal structures

None of the complexes maintain the solvation molecules after the crystallization process. The structure of complex **1**, $(PPh_4)_n${[Rh_2(μ-$O_2CPh)_4$][$Au(CN)_2$]}$_n$, is formed by wavy chains (Fig. 2). In this compound all the Rh–Au–Rh angles are equal (167.77°) whereas two different Rh–N–Au angles of 161.59° and 173.32°, corresponding to two adjacent dirhodium units are observed. The chains are positioned parallel to each other (Fig. 2) with the PPh_4^+ cations placed between them, so that the shortest Au···Au distance found in the crystal structure is as long as 10.735 Å.

As seen, the presence of bulky carboxylate ligands and PPh_4^+ cations plays an important role on the distribution of the formed chains, avoiding the existence of Au···Au interactions. Moreover, the presence of substituents bulkier than a phenyl group in the carboxylate ligands of tetraphenylphosphonium derivatives prevents even the formation of chains in the complex $(PPh_4)_2${Rh_2(μ-$O_2CR)_4$[$Au(CN)_2]_2$} (R

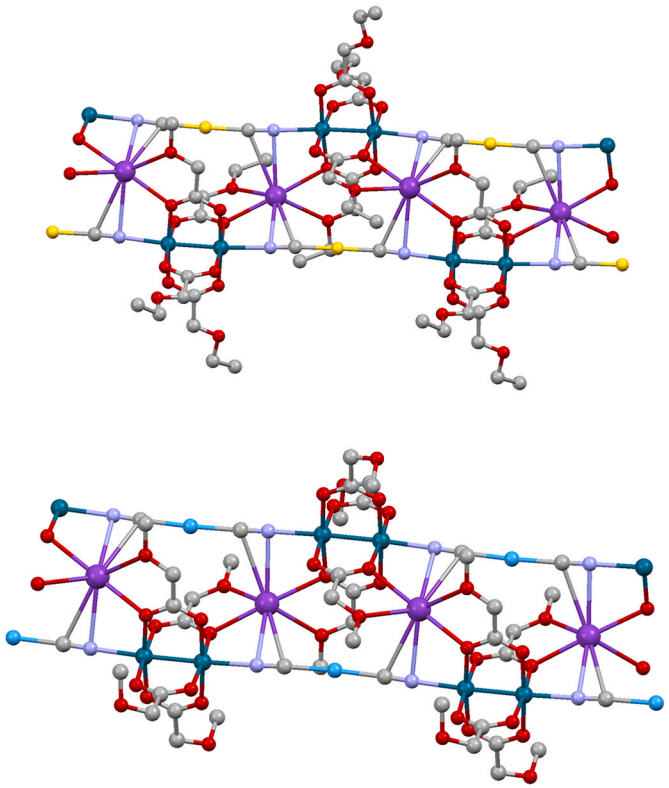

Fig. 3. View of the structures of **2** (top) and **4** (bottom). The code of colors is the same as in Fig. 2. In addition, K atoms are shown in dark purple and Ag atoms are shown in blue. H atoms are omitted for the sake of clarity. (For interpretation of the references to colour in this figure legend, the reader is referred to the Web version of this article.)

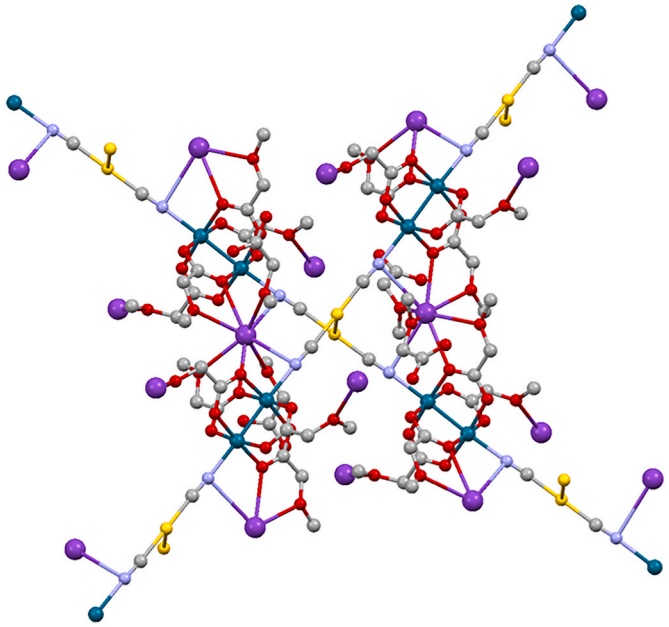

Fig. 4. View of the structure of **3**. The code of colors is the same as in Figs. 2 and 3. H atoms are omitted for the sake of clarity. (For interpretation of the references to colour in this figure legend, the reader is referred to the Web version of this article.)

=C_6H_4–*p*–CMe_3) [37]. Therefore, a change of both carboxylate ligands and counterions was studied to evaluate its effect on the packing in the solid state. The arrangement found in the crystal structure of complex **2**, $K_n\{[Rh_2(\mu\text{-}O_2CCH_2OEt)_4][Au(CN)_2]\}_n$ (Fig. 3, top) is made of one-dimensional chains with Rh–Au–Rh and Rh–N–Au angles of 174.55 and 173.27°, respectively. The K^+ counterion is placed in an octacoordinated environment, connecting two parallel chains, and is coordinated to one oxygen from a carboxylate group (2.672 Å), another oxygen from its ethoxy group (2.831 Å), a carbon (3.312 Å) and a nitrogen (3.078 Å) from the CN group of one chain and the homologues of these four atoms from the adjacent chain. A similar octacoordinated environment for the K^+, involving the CN group, was found in the crystal structure of $K_n\{[Rh_2(\mu\text{-}O_2CMe)_4][Au(CN)_2]\}_n{\cdot}4nH_2O$ [35]. Again, no aurophilic interactions are observed in this structure since the shortest Au···Au distance within the double chains is 8.431 Å while the Au···Au distance between adjacent double chains of different pairs is 8.722 Å. This situation contrast with that observed in a related complex, $K_n\{[Rh_2(\mu\text{-}O_2CEt)_4][Au(CN)_2]\}_n$, formed by wavy chains that are connected through Au···Au interactions (3.328 Å) [35].

When working with the methoxy acetate ligand supporting the dirhodium unit (compounds **3** and **4**), two different metallic linkers were employed to assess the influence of those on the final arrangement, in the solid state, of the complexes. In complex **3** the $[Au(CN)_2]^-$ groups are occupying the axial positions of subsequent dimetallic units, resulting one-dimensional chains. This chains present angles Rh–Au–Rh y Rh–N–Au of 177.16 and 176.97°, respectively, giving almost linear chains. In the solid-state ordering of this compound, one can see the $\{[Rh_2(\mu\text{-}O_2CCH_2OMe)_4][Au(CN)_2]\}_n^-$ chains which are positioned perpendicular to each other with an Au···Au interchain distance of 2.963 Å (Fig. 4). This short Au–Au distance suggests the presence of strong aurophilic interactions. Consequently, the solid is made up of sheets formed by parallel and perpendicular chains joined by aurophilic interactions. This type of interactions appears for distances ranging from 2.8 to 3.5 Å and are key elements to increase structural dimensionality by crystal design in some materials [38]. The lamellae are joined to each other by van der Waals forces and by the K^+ environments. The K^+ cations are located in an octacoordinate environment being coordinated to two nitrogens of the CN groups and 6 oxygens of the methoxyacetates of the four aforementioned chains. The structure of the only related compound that displays aurophilic interactions, $K_n\{[Rh_2(\mu\text{-}O_2CEt)_4][Au(CN)_2]\}_n$, has a remarkably different solid state arrangement. This structure is made of alternating layers of parallel zigzag chains. Au···Au interactions (3.328 Å) are stablished between gold atoms of adjacent layers [35].

In high contrast, when $[CN–Ag–CN]^-$ is used (**4**), the absence of Ag···Ag interactions (8.083 Å) does not allow the chains to be perpendicular to each other and instead, a parallel ordering similar to the one of **2** is observed (Fig. 3, bottom). Therefore, the Au···Au interactions observed in the structure of **3** seem to be a key factor that drives its final packing, while potential weaker Ag···Ag interactions do not have the same effect in the structure of **4**. In this case, the Rh–Ag–Rh angles are 178.37° and 175.64° whereas the Rh–N–Ag angles are 176.64° and 179.95, respectively, so they can be considered pseudolinear chains, which are connected through K^+ ions with a similar coordination environment to that observed in the structure of **2**.

3.3. *Diffuse reflectance and emission studies*

Gold and its chemistry have been extensively studied and reviewed where its luminescent properties have been known since 1970 [41]. The tendency of Au(I) complexes for linear coordination and aurophilicity often leads to aggregation of these linear units into more complicated scaffolds [42,43]. The presence of Au··Au interactions often rise ligand to metal-metal (LMMCT) charge transitions responsible for the emissive behavior of many of these polynuclear aggregates [44]. Indeed, it has been previously studied that variation of the metal−metal distances

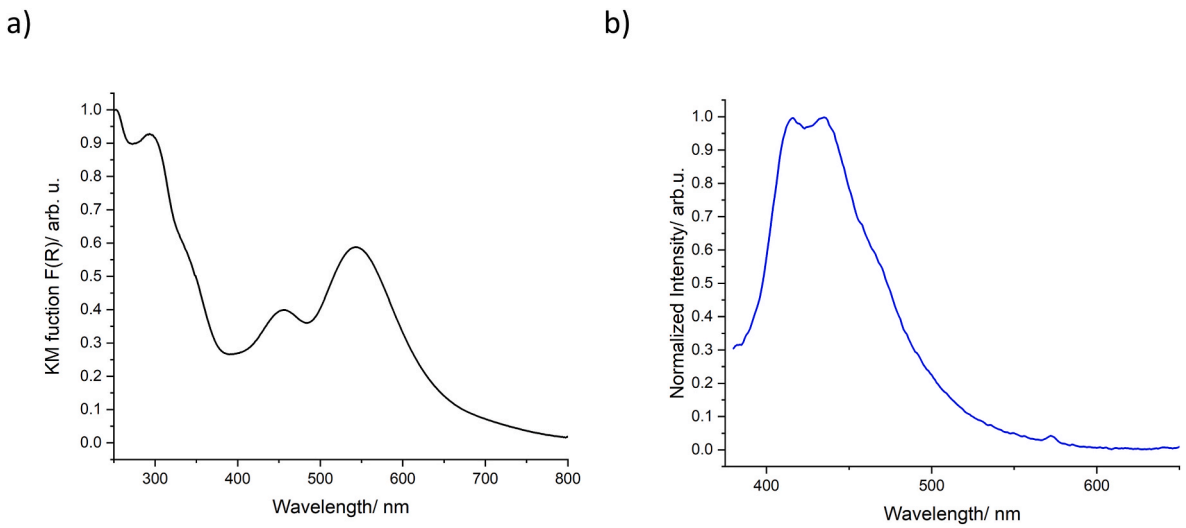

Fig. 5. KM function (a) and emission (λ_{exc} = 350 nm) (b) spectra of complex **3** in the solid state at room temperature.

normally leads to a shift of the emissions spectra [45] if the Au(I) centers are separated by less than 3.6 Å [46].

As seen in the previous sections, compound **3** presents relatively strong aurophilic interactions (Au···Au of 2.963 Å) and therefore, emission properties could be expected. The reflectance and emission properties were studied for this complex in the solid state at room temperature (Fig. 5). The absorption spectrum calculated from the diffuse reflectance spectrum by application of the KM-function, presents three distinguished bands at 300, 450 and 540 nm. Following previously reported works, the first one could be associated to the a metal-to-ligand charge transfer (MLCT) (d → π*) transition from the $[Au(CN)_2]^-$ fragment [47–49]. In contrast, the other two bands could be assigned to transitions involving the Rh_2 scaffold. Particularly the lowest in energy (540 nm, usually referred to as the A band) is associated to a metal based transition $\pi^*(Rh_2) \rightarrow \sigma^*(Rh_2)$ while the third one at higher energies (450 nm, normally referred to as the B band) is assigned to a transition from the same Rh_2 dπ* orbitals to orbitals that are σ-antibonding with respect to the Rh–O bonds of the equatorial carboxylate ligands, $\pi^*(Rh_2) \rightarrow \sigma^*$(Rh–O) [30,50]. Excitation between 290 nm and 350 nm results in a weak emission band centered at 430 nm that could be assigned to the aurophilic $[Au(CN)_2]^-$ units in line with previously studied $[Au(CN)_2]^-$ based compounds [35,47,51] (Fig. S5). The appearance of an artificial structure within this band could be observed due to vibrational structures of Au–Au interactions between the different layers, as has been previously described in the case of 2D-networks [52] or simply by light scattering. This is often observed in the case of solid samples and it has been shown in Fig S6, as by exciting at different wavelengths the scatter bands shifts while the emission band 430 nm (assigned to the aurophilic $[Au(CN)_2]^-$ units) remains constant (Fig. S6). By comparison with our previously reported $K_n\{[Rh_2(\mu\text{-}O_2CEt)_4][Au(CN)_2]\}_n$ [35] with Au···Au interchain distances of 3.328 Å and emission wavelength of 475 nm, a clear blue shift of the emission band is observed in accordance with the shorter aurophilic interactions presented by complex **3**.

4. Conclusions

The reaction of the dirhodium tetracarboxylates $[Rh_2(\mu\text{-}O_2CR)_4(L)_2]$ (R = Ph, CH_2OEt, CH_2OMe), with $[M(CN)_2]^-$ (M = Au, Ag) leads, in all cases, to one-dimensional chains. The arrangement of those in the solid state depends on the nature of the carboxylate ligand, the metal employed as linker and the nature and size of the counterion. From the results obtained in this work it is deduced that to obtain luminiscent properties, in the dicyanoaurate complexes, small carboxylate ligands, as methoxy acetate, and monoatomic counterions, as K^+ must be used. In this case the chains can be ordered close enough to allow Au–Au aurophilic interactions, forming a 2D-network. Thus, only in the case of complex **3** luminescent properties were observed. In contrast, the very similar dicyanoargentato derivative (**4**) does not present Ag–Ag interactions highlighting the influence of the metal on this type of interaction.

CRediT authorship contribution statement

Laura Abad Galán: Writing – review & editing, Writing – original draft, Validation, Investigation, Formal analysis, Conceptualization. **Paula Cruz:** Writing – review & editing, Investigation, Formal analysis. **Estefanía Fernández-Bartolomé:** Writing – review & editing, Investigation, Formal analysis. **Miguel Cortijo:** Writing – review & editing, Writing – original draft, Formal analysis. **Patricia Delgado-Martínez:** Writing – review & editing, Formal analysis. **Rodrigo González-Prieto:** Writing – review & editing, Writing – original draft, Investigation, Formal analysis. **Reyes Jiménez-Aparicio:** Writing – review & editing, Writing – original draft, Validation, Supervision, Methodology, Investigation, Funding acquisition, Formal analysis, Conceptualization. **José L. Priego:** Writing – review & editing, Writing – original draft, Validation, Supervision, Methodology, Investigation, Conceptualization.

Funding

This research was funded by the Spanish Ministerio de Economía y Competitividad (project CTQ2015-63858-P, MINECO/FEDER).

Declaration of competing interest

The authors declare that they have no known competing financial interests or personal relationships that could have appeared to influence the work reported in this paper.

Acknowledgments

The authors are very thankful to the Chemical Optosensors and Applied Photochemistry Group (GSOLFA) and especially, to Prof. Guillermo Orellana Moraleda at Complutense University (Madrid, Spain) for the use of their spectrofluorometer.

Appendix A. Supplementary data

Supplementary data to this article can be found online at https://doi.

org/10.1016/j.polymer.2024.127861.

Data availability

No data was used for the research described in the article.

References

[1] J.R. Long, O.M. Yaghi, The pervasive chemistry of metal–organic frameworks, Chem. Soc. Rev. 38 (2009) 1213–1214, https://doi.org/10.1039/B903811F.

[2] H.-C. Zhou, J.R. Long, O.M. Yaghi, Introduction to metal–organic frameworks, Chem. Rev. 112 (2012) 673–674, https://doi.org/10.1021/cr300014x.

[3] W.L. Leong, J.J. Vittal, One-dimensional coordination polymers: complexity and diversity in structures, properties, and applications, Chem. Rev. 111 (2011) 688–764, https://doi.org/10.1021/cr100160e.

[4] Y. Liu, J. Wu, W. Li, J. Li, H. Han, Z. Song, Responsive metal–organic framework nanocarrier delivery system: an effective solution against bacterial infection, Coord. Chem. Rev. 496 (2023) 215431, https://doi.org/10.1016/j.ccr.2023.215431.

[5] J. Huang, W. Li, X. Bai, F. Xiao, H. Xu, Metal–organic framework detectives meet infectious pathogens: a powerful tool against pandemics, Coord. Chem. Rev. 488 (2023) 215160, https://doi.org/10.1016/j.ccr.2023.215160.

[6] R.M. Almotawa, G. Aljomaih, D.V. Trujillo, V.N. Nesterov, M.A. Rawashdeh-Omary, New coordination polymers of copper(I) and silver(I) with pyrazine and piperazine: a step toward "green" chemistry and optoelectronic applications, Inorg. Chem. 57 (2018) 9962–9976, https://doi.org/10.1021/acs.inorgchem.8b01131.

[7] Y. Wang, S. Bao, R. Li, G. Zhao, Z. Wang, Z. Zhao, Q. Chen, Universal strategy for homogeneously doping noble metals into cyano-bridged coordination polymers, ACS Appl. Mater. Interfaces 7 (2015) 2088–2096, https://doi.org/10.1021/am508246m.

[8] C. Zhang, K. Fan, Y. Chen, Y. Wu, C. Wang, Conjugated coordination polymers as electrodes for rechargeable batteries, ACS Appl. Electron. Mater. 3 (2021) 1947–1958, https://doi.org/10.1021/acsaelm.1c00297.

[9] K.A. McDonald, S. Seth, A.J. Matzger, Coordination polymers with high energy density: an emerging class of explosives, Cryst. Growth Des. 15 (2015) 5963–5972, https://doi.org/10.1021/acs.cgd.5b01436.

[10] F.-X. Xu, Y.-T. Zhou, C.-C. Zhang, X.-Y. Zhang, H.-Y. Wei, X.-Y. Wang, Syntheses, structures, and magnetic properties of three cyano-bridged Fe^{II} –Mo^{III} single-molecule magnets, Inorg. Chem. 62 (2023) 15465–15478, https://doi.org/10.1021/acs.inorgchem.3c01803.

[11] X.-M. Li, C.-F. Wang, Y. Ji, L.-C. Kang, X.-H. Zhou, J.-L. Zuo, X.-Z. You, Heterometallic complexes based on the mixed bridging ligands of tricyanometalate and terephthalate: syntheses, structures, and magnetic properties, Inorg. Chem. 48 (2009) 9166–9173, https://doi.org/10.1021/ic900757s.

[12] J.A. Chipman, J.F. Berry, Paramagnetic metal–metal bonded heterometallic complexes, Chem. Rev. 120 (2020) 2409–2447, https://doi.org/10.1021/acs.chemrev.9b00540.

[13] G. Romo-Islas, J.S. Ward, K. Rissanen, L. Rodríguez, Heterometallic Au(I)–Cu(I) clusters: luminescence studies and $^1O_2$ production, Inorg. Chem. 62 (2023) 8101–8111, https://doi.org/10.1021/acs.inorgchem.3c00046.

[14] A.F. Heyduk, D.J. Krodel, E.E. Meyer, D.G. Nocera, A luminescent heterometallic Dirhodium−Silver chain, Inorg. Chem. 41 (2002) 634–636, https://doi.org/10.1021/ic015562d.

[15] H.K. Yip, H.M. Lin, Y. Wang, C.M. Che, Electronic structure and spectroscopy of luminescent heterobimetallic platinum(II)-Rhodium(I), gold(I)-Rh(I), and silver(I)-Rh(I) complexes, Inorg. Chem. 32 (1993) 3402–3407, https://doi.org/10.1021/ic00068a006.

[16] M.P.S. Rodrigues, A.H.B. Dourado, A.G. Sampaio De Oliveira-Filho, A.P. De Lima Batista, M. Feil, K. Krischer, S.I. Córdoba De Torresi, Gold–rhodium nanoflowers for the plasmon-enhanced CO_2 electroreduction reaction upon visible light, ACS Catal. 13 (2023) 267–279, https://doi.org/10.1021/acscatal.2c04207.

[17] M.P.D.S. Rodrigues, A.H.B. Dourado, L.D.O. Cutolo, L.S. Parreira, T.V. Alves, T.J. A. Slater, S.J. Haigh, P.H.C. Camargo, S.I. Cordoba De Torresi, Gold–rhodium nanoflowers for the plasmon-enhanced hydrogen evolution reaction under visible light, ACS Catal. 11 (2021) 13543–13555, https://doi.org/10.1021/acscatal.1c02938.

[18] R.H. Lam, S.T. Keaveney, B.A. Messerle, I. Pernik, Bimetallic rhodium complexes: precatalyst activation-triggered bimetallic enhancement for the hydrosilylation transformation, ACS Catal. 13 (2023) 1999–2010, https://doi.org/10.1021/acscatal.2c04388.

[19] Y. Liu, L. Li, S. Meng, J. Wang, Q. Xu, P. Ma, J. Wang, J. Niu, Fabrication of polyoxometalate-based metal–organic frameworks integrating paddlewheel $Rh_2(OAc)_4$ for visible-light-driven oxidative coupling of amines, Inorg. Chem. 62 (2023) 12954–12964, https://doi.org/10.1021/acs.inorgchem.3c01749.

[20] T. Murai, W. Lu, T. Kuribayashi, K. Morisaki, Y. Ueda, S. Hamada, Y. Kobayashi, T. Sasamori, N. Tokitoh, T. Kawabata, T. Furuta, Conformational control in dirhodium(II) paddlewheel catalysts supported by chalcogen-bonding interactions for stereoselective intramolecular C–H insertion reactions, ACS Catal. 11 (2021) 568–578, https://doi.org/10.1021/acscatal.0c03689.

[21] Z.J. Garlets, Y.T. Boni, J.C. Sharland, R.P. Kirby, J. Fu, J. Bacsa, H.M.L. Davies, Design, synthesis, and evaluation of extended C_4–symmetric dirhodium tetracarboxylate catalysts, ACS Catal. 12 (2022) 10841–10848, https://doi.org/10.1021/acscatal.2c03041.

[22] B.G. Anderson, D. Cressy, J.J. Patel, C.F. Harris, G.P.A. Yap, J.F. Berry, A. Darko, Synthesis and catalytic properties of dirhodium paddlewheel complexes with tethered, axially coordinating thioether ligands, Inorg. Chem. 58 (2019) 1728–1732, https://doi.org/10.1021/acs.inorgchem.8b02627.

[23] S.A. Hilderbrand, M.H. Lim, S.J. Lippard, Dirhodium tetracarboxylate scaffolds as reversible fluorescence-based nitric oxide sensors, J. Am. Chem. Soc. 126 (2004) 4972–4978, https://doi.org/10.1021/ja038471j.

[24] R.C. Smith, A.G. Tennyson, S.J. Lippard, Polymer-bound dirhodium tetracarboxylate films for fluorescent detection of nitric oxide, Inorg. Chem. 45 (2006) 6222–6226, https://doi.org/10.1021/ic060070s.

[25] M.E. Moragues, J. Esteban, J.V. Ros-Lis, R. Martínez-Máñez, M.D. Marcos, M. Martínez, J. Soto, F. Sancenón, Sensitive and selective chromogenic sensing of carbon monoxide via reversible axial CO coordination in binuclear rhodium complexes, J. Am. Chem. Soc. 133 (2011) 15762–15772, https://doi.org/10.1021/ja206251r.

[26] I. Tolbatov, A. Marrone, Kinetics of reactions of dirhodium and diruthenium paddlewheel tetraacetate complexes with nucleophilic protein sites: computational insights, Inorg. Chem. 61 (2022) 16421–16429, https://doi.org/10.1021/acs.inorgchem.2c02516.

[27] H.T. Chifotides, K.R. Dunbar, Interactions of Metal−Metal-bonded antitumor active complexes with DNA fragments and DNA, Acc. Chem. Res. 38 (2005) 146–156, https://doi.org/10.1021/ar0302078.

[28] D.V. Deubel, Mechanism and control of rare tautomer trapping at a Metal−Metal bond: adenine binding to dirhodium antitumor Agents[1], J. Am. Chem. Soc. 130 (2008) 665–675, https://doi.org/10.1021/ja076603t.

[29] D. Loreto, B. Maity, T. Morita, H. Nakamura, A. Merlino, T. Ueno, Cross-linked crystals of dirhodium tetraacetate/RNase A adduct can Be used as heterogeneous catalysts, Inorg. Chem. 62 (2023) 7515–7524, https://doi.org/10.1021/acs.inorgchem.3c00852.

[30] P. Amo-Ochoa, R. Jiménez-Aparicio, J. Perles, M.R. Torres, M. Gennari, F. Zamora, Structural diversity in paddlewheel dirhodium(II) compounds through ionic interactions: electronic and redox properties, Cryst. Growth Des. 13 (2013) 4977–4985, https://doi.org/10.1021/cg4011532.

[31] Y. Kataoka, N. Yano, T. Shimodaira, Y.-N. Yan, M. Yamasaki, H. Tanaka, K. Omata, T. Kawamoto, M. Handa, Paddlewheel-type dirhodium tetrapivalate based coordination polymer: synthesis, characterization, and self-assembly and disassembly transformation properties, Eur. J. Inorg. Chem. 2016 (2016) 2810–2815, https://doi.org/10.1002/ejic.201600197.

[32] N. Fritsch, C.R. Wick, T. Waidmann, P.O. Dral, J. Tucher, F.W. Heinemann, T. E. Shubina, T. Clark, N. Burzlaff, Multiply bonded metal(II) acetate (rhodium, ruthenium, and molybdenum) complexes with the trans-1,2-bis(N-Methylimidazol-2-yl)ethylene ligand, Inorg. Chem. 53 (2014) 12305–12314, https://doi.org/10.1021/ic501435a.

[33] E.V. Dikarev, R.V. Shpanchenko, K.W. Andreini, E. Block, Jin, M.A. Petrukhina, Powder diffraction study of a coordination polymer comprised of rigid building blocks: $[Rh_2(O_2CCH_3)_4\text{-}\mu^2\text{-}Se_2C_5H_8\text{-}Se,Se']_\infty$, Inorg. Chem. 43 (2004) 5558–5563, https://doi.org/10.1021/ic049497u.

[34] Y. Kim, S.-J. Kim, A.J. Lough, New dirhodium(II,II) carboxylates with 2,6-bis(N′-1,2,4-Triazolyl)Pyridinato ligand (Btp), Polyhedron 20 (2001) 3073–3078, https://doi.org/10.1016/S0277-5387(01)00919-6.

[35] P. Amo-Ochoa, S. Delgado, A. Gallego, C.J. Gómez-García, R. Jiménez-Aparicio, G. Martínez, J. Perles, M.R. Torres, Structure and properties of one-dimensional heterobimetallic polymers containing dicyanoaurate and dirhodium(II) fragments, Inorg. Chem. 51 (2012) 5844–5849, https://doi.org/10.1021/ic3004307.

[36] P. Cruz, E. Fernandez-Bartolome, M. Cortijo, P. Delgado-Martínez, R. González-Prieto, J.L. Priego, M.R. Torres, R. Jiménez-Aparicio, Synthesis and structural characterization of a series of one-dimensional heteronuclear dirhodium-silver coordination polymers, Polym. 11 (2019) 111, https://doi.org/10.3390/polym11010111.

[37] E. Fernandez-Bartolome, P. Cruz, L.A. Galán, M. Cortijo, P. Delgado-Martínez, R. González-Prieto, J.L. Priego, R. Jiménez-Aparicio, Heteronuclear dirhodium-gold anionic complexes: polymeric chains and Discrete Units, Polym. 12 (2020) 1868, https://doi.org/10.3390/polym12091868.

[38] M.J. Katz, K. Sakai, D.B. Leznoff, The Use of aurophilic and other metal–metal interactions as crystal Engineering design elements to increase structural dimensionality, Chem. Soc. Rev. 37 (2008) 1884–1895, https://doi.org/10.1039/B709061G.

[39] K. Nakamoto, Infrared and Raman Spectra of Inorganic and Coordination Compounds, sixth ed., Wiley, Hoboken, N.J, 2009, 978-0-471-74339-2.

[40] M.C. Barral, R. Jiménez-Aparicio, J.L. Priego, E.C. Royer, F.A. Urbanos, Liquid Secondary ion mass Spectrometric study of Diruthenium(II,III) complexes, Inorg. Chim. Acta. 277 (1998) 76–82, https://doi.org/10.1016/S0020-1693(97)06125-2.

[41] R.F. Ziolo, S. Lipton, Z. Dori, The photoluminescence of phosphine complexes of d^{10} metals, J. Chem. Soc. D 1124 (1970), https://doi.org/10.1039/c29700001124.

[42] X. He, V.W.-W. Yam, Luminescent gold(I) complexes for chemosensing, Coord. Chem. Rev. 255 (2011) 2111–2123, https://doi.org/10.1016/j.ccr.2011.02.003.

[43] H. Schmidbaur, A. Schier, Aurophilic interactions as a subject of current research: an up-date, Chem. Soc. Rev. 41 (2012) 370–412, https://doi.org/10.1039/C1CS15182G.

[44] T.P. Seifert, V.R. Naina, T.J. Feuerstein, N.D. Knöfel, P.W. Roesky, Molecular gold strings: aurophilicity, luminescence and structure–property correlations, Nanoscale 12 (2020) 20065–20088, https://doi.org/10.1039/D0NR04748A.

[45] N.L. Coker, J.A. Krause Bauer, R.C. Elder, Emission energy correlates with inverse of Gold−Gold distance for various $[Au(SCN)_2]^-$ salts, J. Am. Chem. Soc. 126 (2004) 12–13, https://doi.org/10.1021/ja037012f.

[46] A. Bondi, Van der Waals volumes and radii, J. Phys. Chem. 68 (1964) 441–451, https://doi.org/10.1021/j100785a001.
[47] F. Baril-Robert, X. Li, M.J. Katz, A.R. Geisheimer, D.B. Leznoff, H. Patterson, Changes in electronic properties of polymeric one-dimensional {[$M(CN)_2$]$^-$}n (M = Au, Ag) chains due to neighboring closed-shell Zn(II) or open-shell Cu(II) ions, Inorg. Chem. 50 (2011) 231–237, https://doi.org/10.1021/ic101841a.
[48] S.K. Chastain, W.R. Mason, Electronic and magnetic circular dichroism spectra of linear two-coordinate gold(I) complexes of alkyl isocyanide or trialkyl phosphite ligands, Inorg. Chem. 21 (1982) 3717–3721, https://doi.org/10.1021/ic00140a024.
[49] M.M. Savas, W.R. Mason, Electronic and MCD spectra of linear two-coordinate dihalo-, halo(Trialkylphosphine)-, and bis(Triethylphosphine)Gold(I) complexes, Inorg. Chem. 26 (1987) 301–307, https://doi.org/10.1021/ic00249a018.
[50] Y. Kataoka, Y. Kitagawa, T. Saito, Y. Nakanishi, K. Sato, Y. Miyazaki, T. Kawakami, M. Okumura, W. Mori, K. Yamaguchi, Theoretical study of absorption spectrum of dirhodium tetracarboxylate complex [$Rh_2(CH_3COO)_4(H_2O)_2$] in aqueous solution revisited, Supramol. Chem. 23 (2011) 329–336, https://doi.org/10.1080/10610278.2010.534553.
[51] M.L. Brown, J.S. Ovens, D.B. Leznoff, Dicyanoaurate-based heterobimetallic uranyl coordination polymers, Dalton Trans. 46 (2017) 7169–7180, https://doi.org/10.1039/C7DT00942A.
[52] T. Kitazawa, K. Hiruma, H. Sato, K. Tamura, A. Yamagishi, An emitting hofmann-type compound: evidence for interlayer aurophilic interactions, Dalton Trans. 42 (2013) 16680, https://doi.org/10.1039/c3dt52303a.